Cellular Signalling 62 (2019) 109331

Contents lists available at ScienceDirect

Cellular Signalling

journal homepage: www.elsevier.com/locate/cellsig

Inhibition of 4E-BP1 phosphorylation promotes tubular cell escaping from G2/M arrest and ameliorates kidney fibrosis

Xiaoli Sun[a,1], Wei Wei[a,1], Jiafa Ren[a,1], Yan Liang[a], Mingjie Wang[a], Yuan Gui[a], Xian Xue[a], Jianzhong Li[b,*], Chunsun Dai[a,*]

[a] Center for Kidney Disease, The Second Affiliated Hospital of Nanjing Medical University, 262 North Zhongshan Road, Nanjing, Jiangsu 210003, People's Republic of China

[b] Department of Nephrology, The First Affiliated Hospital of Soochow University, Suzhou, Jiangsu 215006, People's Republic of China

ARTICLE INFO

Keywords:
mTORC1
4E-BP1
G2/M arrest
Tubular epithelial cells
Kidney fibrosis

ABSTRACT

Upon occurrence of kidney injury, tubular cells arrested in G2/M stage may promote interstitial fibroblast activation and kidney fibrosis through producing large amounts of pro-fibrotic cytokines. MTORC1 signaling is essential for controlling cell growth, however, the role and mechanisms for mTORC1 in regulating tubular cell cycle progression during kidney fibrosis are not clear. Here we reported that p-S6 abundance was increased at 15 min, reached peak at 1 h and declined from 3 h to 24 h, while the abundance of p-4E-BP1 and p-Histone H3 was increased from 15 min to 24 h in tubular epithelial cells at the similar pattern after serum stimulation. The phosphorylation of 4E-BP1 was prohibited in NRK-52E cells by the transfection of 4E-BP1 plasmid with four phospho-sites mutation (4E-BP1A4). 4E-BP1A4 transfection led to less G2/M cell arrest as well as the production of pro-fibrotic cytokine and extracellular matrix in NRK-52E cells. In addition, aristolochic acid (AA)-induced tubular cell G2/M arrest induced by treatment was also largely attenuated in NRK-52E cells transfected with 4E-BP1A4. In mouse kidneys with UUO nephropathy, p-4E-BP1 abundance was markedly elevated in the mitotic tubular cells. Therefore, these data indicates that suppressing 4E-BP1 phosphorylation may inhibit tubular cell G2/M-arrest and kidney fibrosis.

1. Introduction

Kidney tubulointerstitial fibrosis (TIF) is one of the major pathological features of chronic kidney diseases [1]. TIF development and progression are complex processes that involve many different cell types, including epithelial [2], myofibroblasts [3], inflammatory cells [4] and endothelia [5]. The proximal tubular has long been regarded as a target of kidney injury, but emerging evidence suggests that it also plays a prominent role in the development and progression of TIF [6].

Renal injury alters the epithelial cell cycle, which promotes TIF progression and the transition from acute kidney injury (AKI) to chronic kidney disease (CKD). During injury, some epithelial cells arrest in G2/M under the regulation of a JNK-dependent pathway, leading to increased production of pro-fibrotic cytokines, such as TGF-β and CTGF [7,8]. In addition, some obtained from the previous studies show that cell cycle regulatory proteins can affect the severity of acute ischemic or cisplatin-induced toxic kidney injury [9,10].

Mammalian target of rapamycin complex 1 (mTORC1) controls cell growth, cell cycling, cell proliferation, metabolism, apoptosis, autophagy, and angiogenesis [11,12]. mTORC1 regulates these processes mainly through ribosomal protein S6 kinase (S6K) and eukaryotic translation initiation factor 4E (eIF4E)-binding protein 1 (4E-BP1) [11,12]. In mouse embryonic fibroblasts, S6Ks play a key role in the control of cell size, and 4E-BP1 is responsive for the proliferation [13]. Moreover, when p-4E-BP1 and p-S6 are inhibited by rapamycin in renal carcinoma cells, the cell cycle is altered [14]; however, for tubular epithelial cells, the function of S6K and 4E-BP1 in cell proliferation and cell cycle needs to be further studied.

Our previous report demonstrated that mTORC1 signaling in fibroblasts had an important role in several kidney diseases and contributed to the development of TIF [15]. In mice with fibroblast-specific deletion of Tsc1 [15], the activation of mTORC1 signaling was

Abbreviations: TIF, tubulointerstitial fibrosis; AA, aristolochic acid; AKI, acute kidney injury; CKD, chronic kidney disease; mTORC1, mammalian target of rapamycin complex 1

* Corresponding authors.
E-mail addresses: ljzsnk@hotmail.com (J. Li), daichunsun@njmu.edu.cn (C. Dai).

[1] These authors contributed equally to this work.

https://doi.org/10.1016/j.cellsig.2019.05.016
Received 29 December 2018; Received in revised form 29 May 2019; Accepted 29 May 2019
Available online 30 May 2019

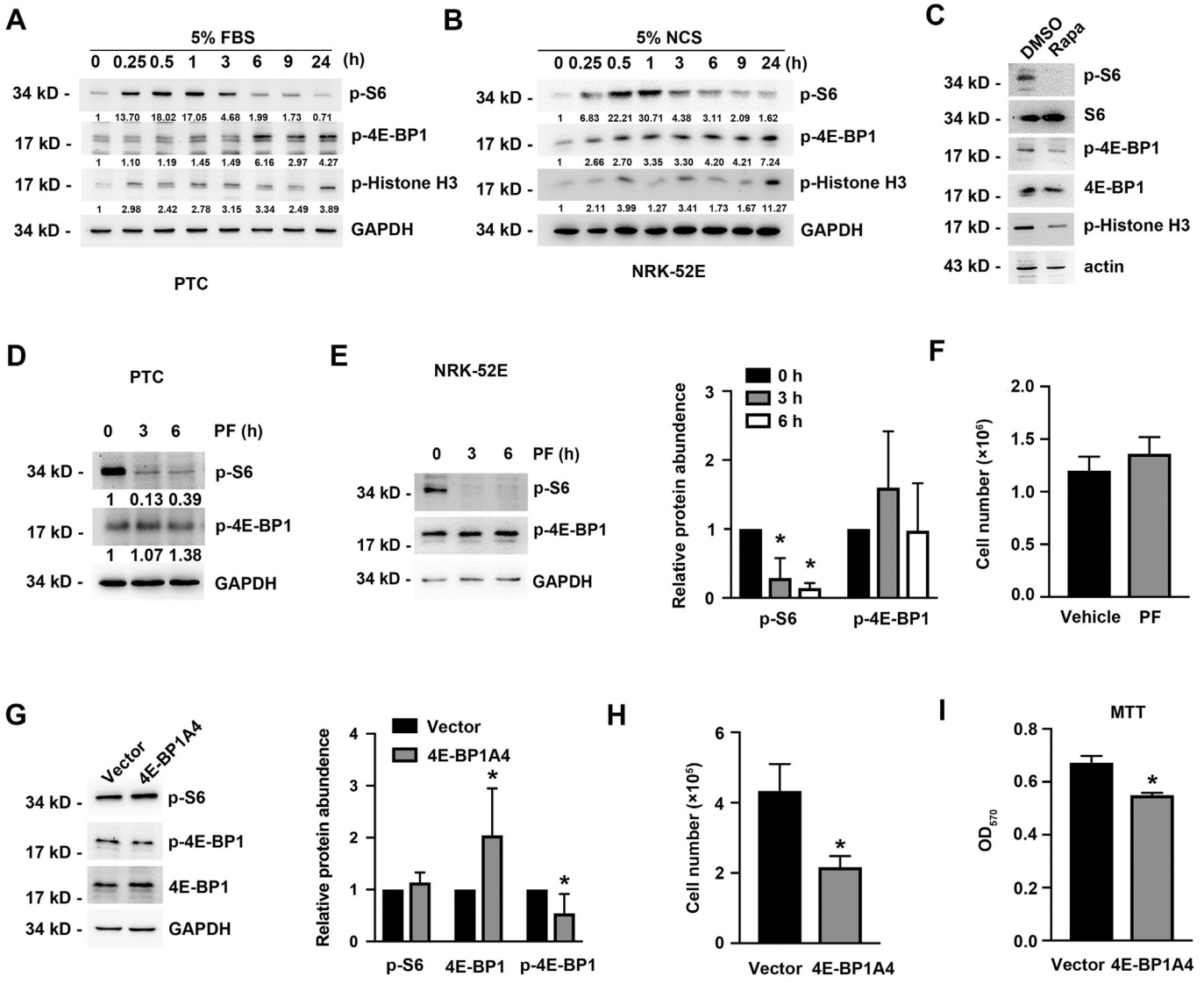

Fig. 1. p-4E-BP1 regulated the tubular epithelia cell proliferation. A-B, PTCs and NRK-52E cells were treated with 5% FBS or 5% NCS for different time duration, western blotting showed the protein expression pattern of mTORC1 pathway. The semi-quantitative analysis was shown below the band. p-S6, p-4E-BP1 and p-Histone H3 bands were corrected with the intensity of the GAPDH control. C, NRK-52E cells were treated with 5 nM Rapamycin for 24 h, western blotting assay showed the mTORC1 pathway protein expression. D-E, PTCs and NRK-52E cells were treated with S6K inhibitor PF-4708671 for different time duration, western blotting assay showed mTORC1 pathway protein expression, quantitative analysis for NRK-52E cells was shown in the right panel of E. * $P < .05$ versus cells treated with DMSO, $n = 3$. F, Cell number was counted when PF was added for 24 h in NRK-52E cells. G-I, The 4E-BP1 mutant 4E-BP1A4 (T37A/T46A/S65A/T70A) was transfected into NRK-52E cells for 24 h, western blotting assay (left panel) and quantitative analysis (right panel) showed the mTORC1 pathway protein expression (G), cell number was showed by counted (H) and MTT assay (I). * $P < .05$ versus cells transfected with vector, n = 3.

significantly increased in kidney interstitial fibroblasts. Inhibition of mTORC1 signaling with rapamycin decreased the phosphorylation of S6K and 4E-BP1 hence attenuating renal fibrosis. mTORC1 in tubular cells regulates endocytosis and nutrient transport, maintains renal tubular homeostasis. mTORC1-deficient mice showed a significantly reduced tubular cell proliferative response after I/R injury [16,17]. However, the role of mTORC1 signaling in epithelial cell on renal fibrosis remains largely unknown. Additionally, in renal carcinoma cells, rapamycin causes a G2/M cell number reduction and cell proliferation suppression [14], providing a probability that inhibition of mTORC1 signaling in epithelial cells may attenuates TIF.

Here, we found that 4E-BP1, rather than p-S6, downstream of mTORC1 signaling regulates cell proliferation in NRK-52E cells. Decreased phosphorylation of 4E-BP1 contributes to epithelial escaping from G2/M arrest, and thereby causing decreased pro-fibrotic cytokines production.

2. Materials and methods

2.1. Mice and animal models

Male C57BL/6 mice and CD1 mice weighing ~18–22 g were acquired from the specific pathogen-free laboratory animal center of Nanjing Medical University and maintained according to the guidelines of the Institutional Animal Care and Use Committee at Nanjing Medical University. UUO was performed as previously reported [18]. The mice received an intraperitoneal injection of 0.75% pentobarbital sodium (0.1 ml/10 g). An incision was made 0.5 cm at the left rib on the back, and the left kidney and ureter were located and isolated with blunt dissection. The left ureter was clamped with tissue and hemostat in the upper and middle segments. After ligation at both ends, the left ureter between ligated sutures was incised and removed. In sham groups, the abdominal cavity was opened but no tissue was removed. Kidneys were

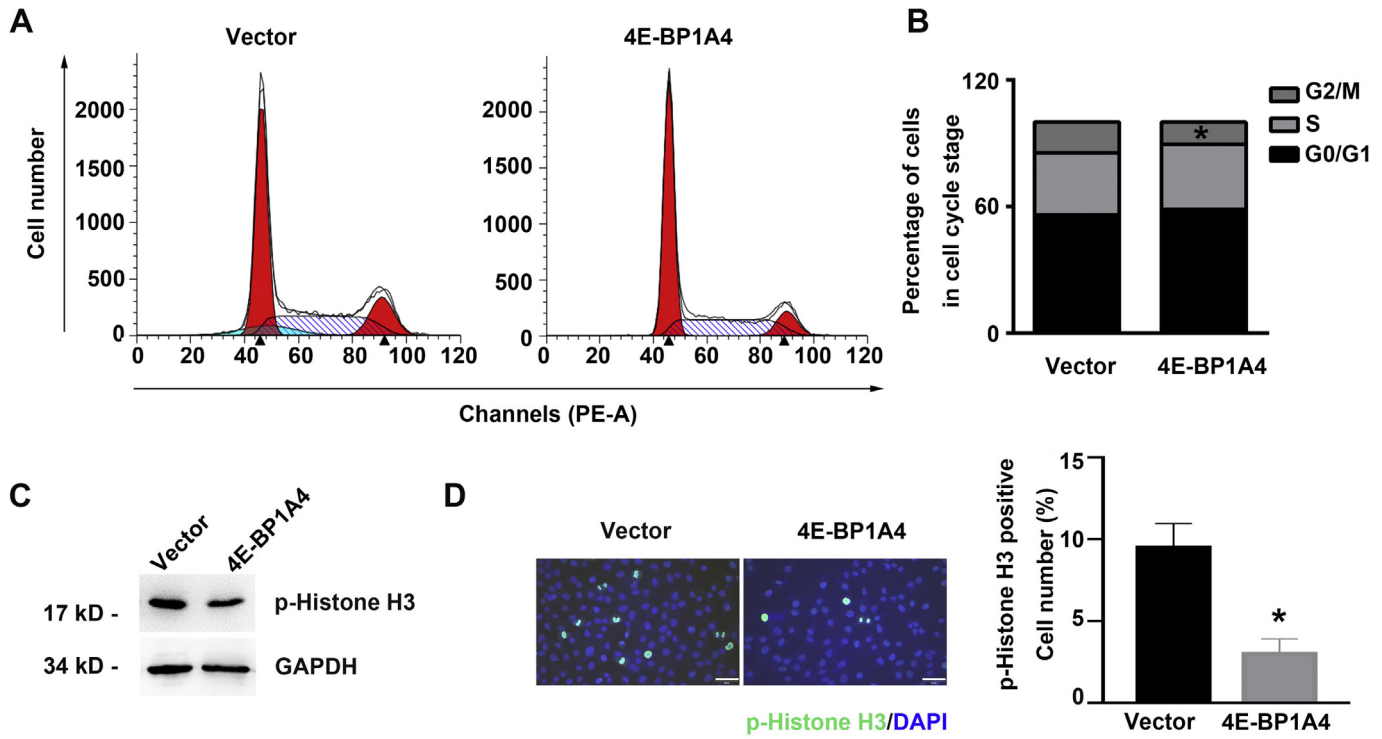

Fig. 2. The 4E-BP1 mutant affected the cell cycle of NRK-52E cells. A-D, Transfected the 4E-BP1A4 into NRK-52E cells for 24 h, the cells were then fixed, permeabilized and analyzed by flow cytometry to detect cell cycle distribution (A), and the histograms represent the distribution of cells cycle (B). $^{*}P < .05$ versus cells transfected with vector, n = 3. C, Western blotting assay showed the p-Histone H3 level with or without 4E-BP1A4 overexpression. D, Representative immunofluorescence staining images (left panel) and quantitative analysis (right panel) showed mitosis cell number with or without 4E-BP1A4 overexpression. $^{*}P < .05$ versus cells transfected with vector, $n = 4$. Scale bar, 50 μm.

harvested at days 0, 3, 7, and 14 after UUO. One portion of the kidney was fixed in 10% phosphate-buffered formalin, followed by paraffin embedding for histological and immunohistochemical staining. Another portion was immediately frozen in Tissue-Tek optimum cutting temperature compound (Sakura Finetek, Torrance, CA) for cryosection. The remaining kidney tissue was snap-frozen in liquid nitrogen and stored at −80 °C for extraction of RNA and protein.

2.2. Cell culture and treatment

Primary tubular epithelial cells (PTC) from mouse kidneys were harvested as previously reported [19]. Briefly, kidneys were surgically removed from anesthetized male C57BL/6 mice (2 weeks old). The renal cortices were sliced, mined and digested in high Krebs-Henseleit-saline (KHS) buffer containing 0.5 mg/ml type collagenase II. Highly purified proximal tubules were maintained in DMEM-F-12 medim supplemented with 1× insulin-transferrin-selenium, 1× MEM non-essential amino acids, 0.1 μM hydrocortisone, 1% (vol/vol) antibiotics (100 IU/ml penicillin and 100 μg/ml streptomycin), 10% (vol/vol) FBS. The cells were seeded on six-well culture plates to 60–70% confluence in complete medium containing 10% FBS for 16 h and then changed to serum-free medium after washing twice with serum-free medium. 5% FBS or PF-4708671 (Sigma-Aldrich, USA) was added to the serum-free medium for various periods of time.

NRK-52E cells were cultured in DMEM-F-12 containing 10% (vol/vol) NCS (Invitrogen, Grand Island, NY) and 1% (vol/vol) antibiotics (100 U/ml penicillin and 100 μg/ml streptomycin) at 37 °C in 5% CO_2. The medium was changed every other day. The cells were seeded on six-well culture plates to 60–70% confluence in complete medium containing 10% NCS for 16 h and then changed to serum-free medium after washing twice with serum-free medium. 5% NCS was added to the serum-free medium for various periods of time. 4E-BP1 mutant 4E-BP1A4 (T37A/T46A/T70A/S65A, GENEWIZ, Suzhou, China) was transfected into NRK-52E cells using Lipofectamine 2000 reagent (Invitrogen) according to the manufacturer's instruction. PF-4708671was added to serum-free medium for various periods of time. Cells were incubated in DMEM medium containing 0.2% NCS for 24 h and treated with 2 g/ml aristolochic acid (AA, cat: A9451, Sigma-Aldrich, USA) for 48 h, then transfected with 4E-BP1A4 for another 24 h.

2.3. Histology and immunohistochemistry

Kidney samples were fixed in 10% neutral formalin and embedded in paraffin. 3 μm thick sections were used for periodic acid-Schiff and Masson staining. For immunohistochemical staining, paraffin-embedded kidney sections were deparaffinized, hydrated, and antigen-retrieved, and endogenous peroxidase activity was quenched by 3% H_2O_2. Sections were then blocked with 10% normal donkey serum, followed by incubation with anti-p-4E-BP1 (cat: 2855 s, Cell Signaling Technology, USA) overnight at 4 °C. After incubation with secondary antibody for 1 h, sections were incubated with ABC reagents for 1 h at room temperature before being subjected to substrate 3-amino-9-ethylcarbazole. Histochemical staining photographs were taken under a photon microscope (Olympus BX53, Japan).

2.4. Immunofluorescence staining

NRK-52E cells cultured on coverslips were washed with cold PBS and fixed with cold methanol:acetone (1:1) for 10 min at −20 °C. After three extensive washings with PBS, cells were treated with 0.1% Triton X-100 for 5 min, blocked with 2% normal donkey serum in PBS buffer for 40 min at room temperature, and incubated with the following antibodies: anti–p-Histone H3 (cat: ab14955, Abcam, USA).

Kidney cryosections at 3 μm thickness were fixed for 15 min with 4% paraformaldehyde followed by permeabilization with 0.2% Triton

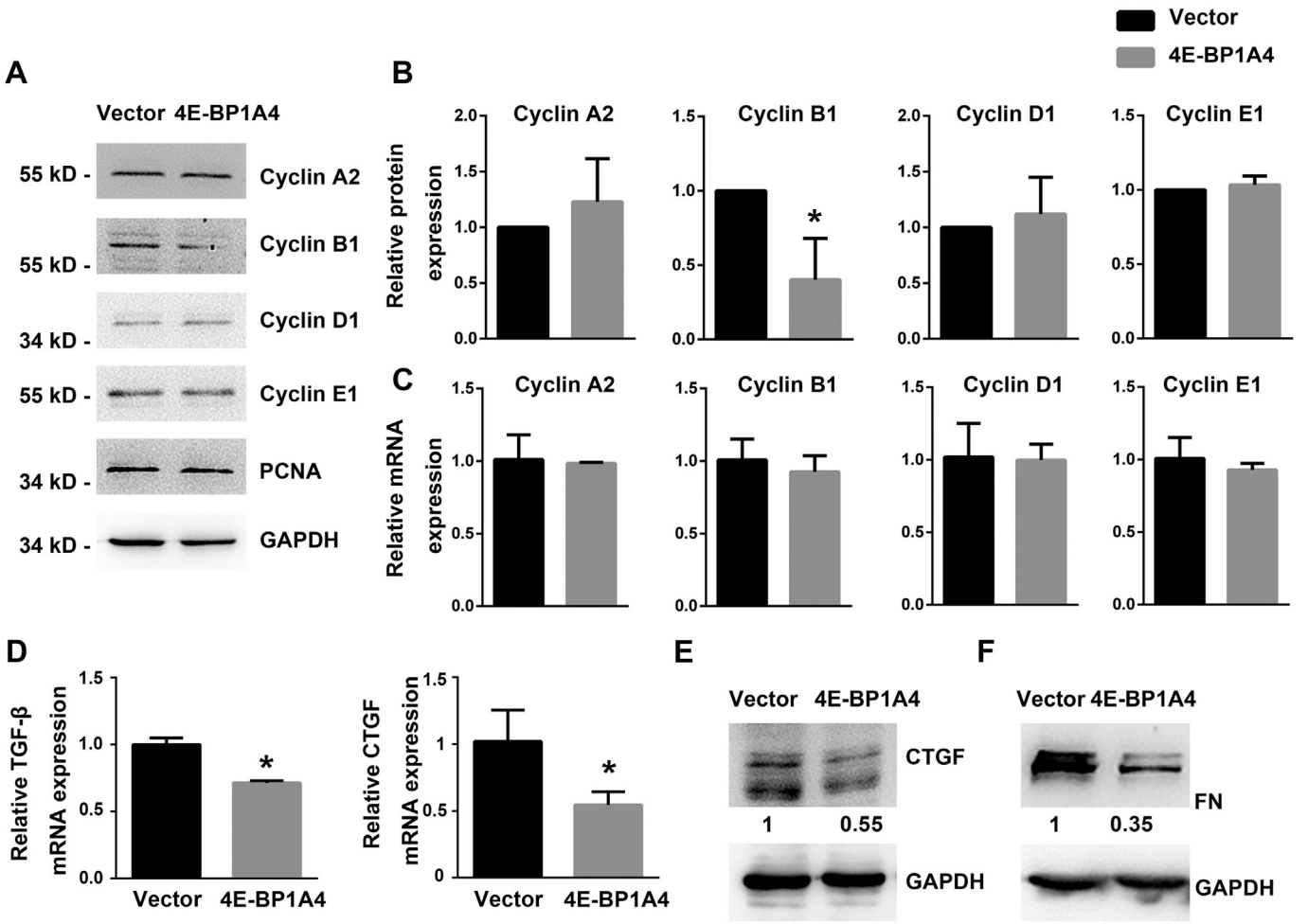

Fig. 3. The 4E-BP1 mutant inhibited the cyclin proteins and pro-fibrotic cytokines expression of NRK-52 cells. Transfected the 4E-BP1A4 into NRK-52E cells for 24 h, western blotting assay (A) and quantitative analysis (B) showed the cyclin proteins expression in NRK-52E cells with or without 4E-BP1A4 overexpression. Cyclin A2, Cyclin B1, Cyclin D1 and Cyclin E1 bands were corrected with the intensity of the GAPDH control. C, Real-time PCR analysis showing the mRNA abundance for cyclins in NRK-52E cells with or without 4E-BP1A4 overexpression. D, Real-time PCR analysis showing the mRNA abundance for pro-fibrotic cytokines expression in NRK-52E cells with or without 4E-BP1A4 overexpression. E and F, Western blotting assay showed the pro-fibrotic cytokine CTGF and extracellular matrix fibronectin (FN) expression in NRK-52E cells with or without 4E-BP1A4 overexpression. The semi-quantitative analysis was shown below the band. CTGF and FN bands were corrected with the intensity of the GAPDH control. * $P < .05$ versus cells transfected with vector, n = 3.

X-100 in PBS for 5 min at room temperature. After blocking with 2% donkey serum for 60 min, slides were immune stained with the following antibodies: anti-p-4E-BP1 and anti-p-Histone H3.

Immunofluorescence-labeled samples were examined using a fluorescent microscope (Olympus BX53, Japan).

2.5. Cell cycle analysis

NRK-52E cells were harvested with trypsin-EDTA, centrifuged into a pellet, and rinsed with phosphate-buffered saline (PBS). Then, 80% ethanol was added, and the cells were incubated on ice for 1 h. The cells were washed with PBS, re-suspended in cell cycle staining buffer (cat: CCS01, MULTI SCIENCES, China), and incubated at room temperature for 30 min, and analyzed on BD Canto II Flow Cytometer with FlowJo software.

2.6. RNA isolation and real-time quantitative RT-PCR

Total RNA was extracted using Trizol reagent (Invitrogen) according to the manufacturer's instructions. cDNA was synthesized using 1 μg of total RNA, HiScript II One Step RT-PCR Kit (Vazyme, Nanjing, China), and oligo (dT) 12–18 primers. Gene expression was measured by real-time PCR using real-time PCR Master Mix reagents (Vazyme, Nanjing, China) and 7300 real-time PCR system (Applied Biosystems, Foster City, CA). For real-time PCR analysis, the relative amount of mRNA or gene to internal control was calculated using the eq. 2ΔCT, in which ΔCT = CT gene-CT control. TGF-β: sense, GAGCCCGAAGCGGACTA CTA; antisense, GTTGTTGCGGTCCACCATT; CTGF: sense, CGCCAACC GCAAGATTG; antisense, ACACGGACCCACCGAAGAC; GAPDH: sense, GATGACATCAAGAAGGTGGTGA; antisense, ACCCTGTTGCTGTAGCCA TATTC.

2.7. Statistical analysis

Analysis of variance was used to compare data among groups. Student's *t*-test was used to determine a significant difference between two groups. A P value of < 0.05 was considered significant. The results are presented as means ± S.D.

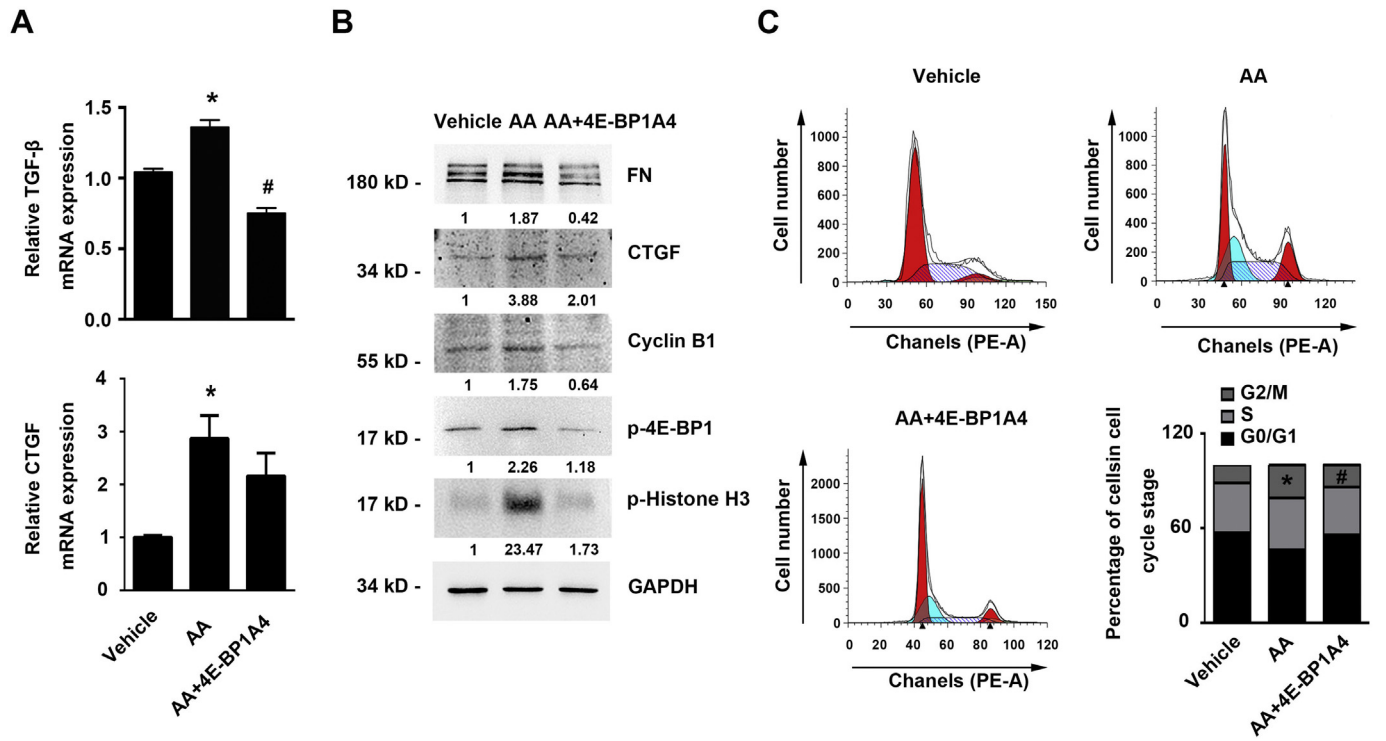

Fig. 4. The 4E-BP1 mutant rescued the effect induced by AA in NRK-52E cells. NRK-52E cells treated with 2 μM AA for 48 h, and transfected with or without 4E-BP1A4 for 24 h. A, Real-time PCR analysis showing the mRNA abundance for TGF-β and CTGF in NRK-52E cells, $^{*}P < .05$ versus cells treated with vehicle alone, n = 3; $^{\#}P < .05$ versus cells treated with AA, n = 3. B, Western blotting assay showing the protein expression of FN, CTGF, Cyclin B1 and p-Histone H3. The semi-quantitative analysis was shown below the band. FN, CTGF, Cyclin B1, p-4E-BP1 and p-Histone H3 bands were corrected with the intensity of the GAPDH control. C, Cell cycle analysis by propidium iodide staining and flow cytometry and the histograms represent the distribution of cells cycle in NRK-52E cells at baseline and after treatment with AA for 48 h, with or without 4E-BP1A4 overexpression. $^{*}P < .05$ versus cells treated with vehicle alone, n = 3; $^{\#}P < .05$ versus cells treated with AA, n = 3.

3. Results

3.1. Suppressing 4E-BP1 phosphorylation decreases tubular epithelial cell proliferation

mTORC1 signal pathway is involved in many cell pathology processes, including metabolism, growth and proliferation. 4E-BP1 and S6K1 are the two important downstream targets of mTORC1. To determine the effect of 4E-BP1 and S6K1 on proliferation in epithelial cells, the serum was used to promote cell proliferation. Primary tubular epithelia cells (PTC) and NRK-52E cells were treated with 5% FBS and 5% NCS, respectively, for different time duration. In PTCs, p-S6 level was induced at as early as 15 min, reached the peak from 30 min to 1 h, and declined at 3 h after treatment. The abundance of p-4E-BP1 continuously increased from 15 min to 24 h, and the mitosis marker p-Histone H3 (Ser10) abundance was significantly induced after 24 h (Fig. 1A). Similar results were observed in NRK-52E cells. The treatment of 5% NCS increased the level of p-4E-BP1 from 30 min to 24 h, and the abundance of p-Histone H3 was significantly increased after 24 h (Fig. 1B). These results indicated that p-4E-BP1 was associated with the proliferation of tubular epithelial cell.

To further investigate the function of mTORC1 on tubular epithelial cell proliferation, we treated NRK-52E cells with 5 nM rapamycin for 24 h to block the mTORC1. It was observed that the level of p-Histone H3 was reduced by rapamycin, and the abundance of p-S6 and p-4E-BP1 were both reduced by rapamycin as well (Fig. 1C). It is difficult to distinguish their role in the proliferation of p-S6 and p-4E-BP1, and hence the S6K1 inhibitor PF-4708671 was used to block the phosphorylation of S6. The 4E-BP1 mutant with all four phospho-sites mutated-Thr37/46/70 and mutated-Ser65 (4E-BP1A4) were used to downregulate the phosphorylation of 4E-BP1. As shown in Fig. 1D–E, whether in PTCs or in NRK-52E cells, the treatment of 10 μM PF-4708671 at 3 h significantly inhibited the phosphorylation of S6 protein. Overexpression of 4E-BP1A4 in NRK-52E cells for 24 h reduced the abundance of phosphorylated 4E-BP1 and cell number, but did not reduced the phosphorylation of p-S6. Taken together, these results indicate that rather than p-S6, 4E-BP1 is responsible for the tubular epithelial cells proliferation.

3.2. Tubular epithelia cells transfected with dominant negative 4E-BP1 mutant reduces cell number in G2/M phase

To investigate the mechanisms of 4E-BP1 affects cell proliferation, we detected the cell cycle distribution of tubular epithelial cells after 4E-BP1A4 overexpression. We transfected NRK-52E cells with 4E-BP1A4 for 24 h, the percentage of cells in G2/M was significantly reduced (Fig. 2A and B), the level of p-Histone H3 was decreased too (Fig. 2C). Immunofluorescent staining results showed that the number of p-Histone H3 positive cells were markedly reduced after 4E-BP1A4 overexpression (Fig. 2D). So, these data indicate that 4E-BP1 regulates tubular epithelial cells proliferation by affecting the cell cycle G2/M phase.

To further evaluate the effect of 4E-BP1 on cell cycle, the cyclins were detected. Fig. 3A and B show that 4E-BPA4 significantly decreased Cyclin B1 in NRK-52E cells, while it had little effect on Cyclin A2, Cyclin D1 and Cyclin E1 protein level. In addition, 4E-BP1A4 didn't affect the transcription of Cyclin B1(Fig. 3C). It is well known that Cyclin B was reduced during mitotic slippage, so it is possible that 4E-BP1A4 promotes the mitotic slippage process via promoting the reduction of Cyclin B1.

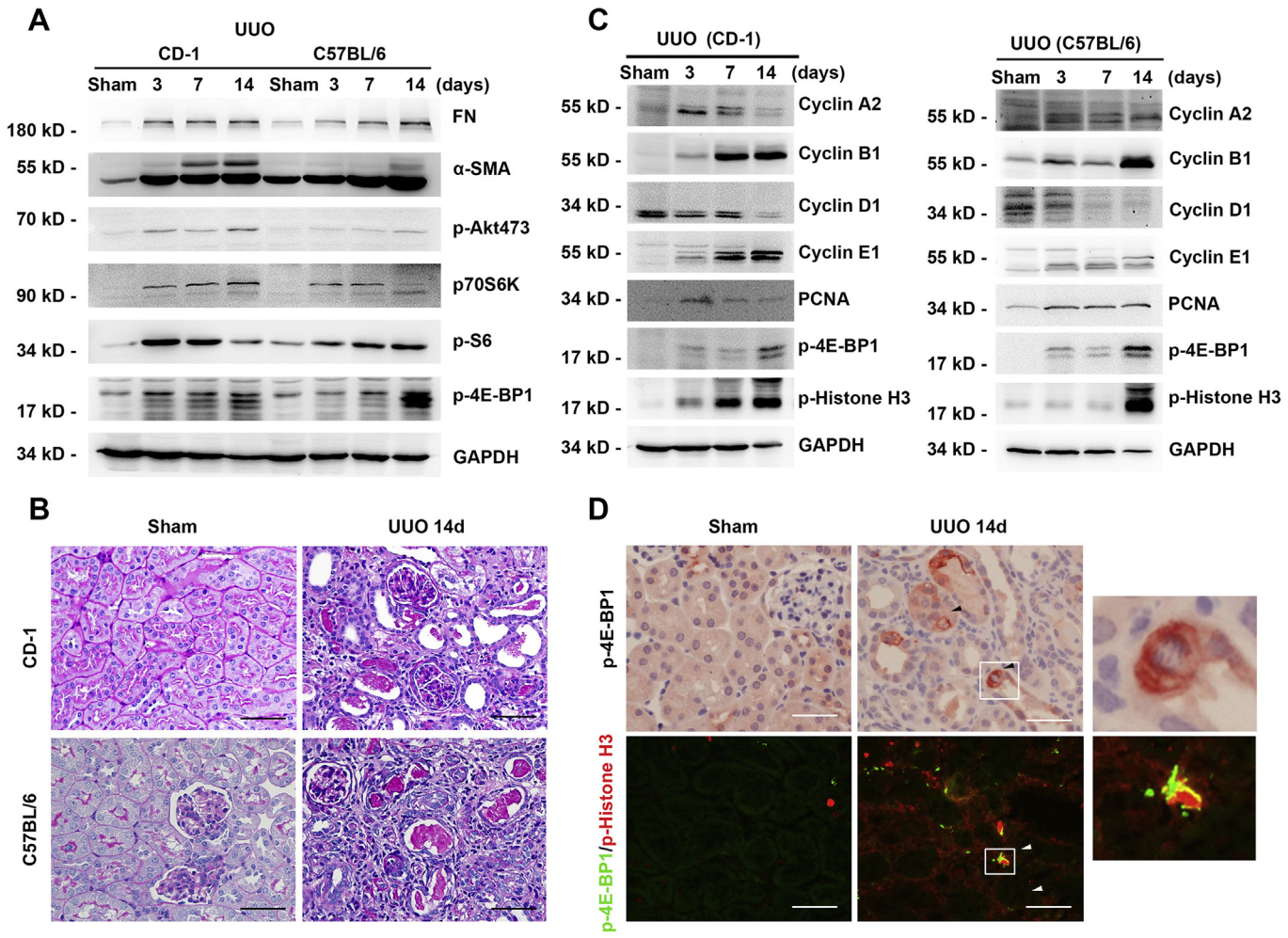

Fig. 5. 4E-BP1 was activated in the tubular cells from the fibrotic kidney with UUO nephropathy. A, Western blotting analyses showing the induction of mTORC1, mTORC2 signaling and extracellular matrix in kidneys at days 3, 7 and 14 after UUO compared with sham control from CD-1 and C57BL/6 mice, respectively. B, Representative micrographs for periodic acid–Schiff (PAS) staining in kidney tissues from CD-1 and C57BL/6 mice, respectively. Scale bar, 50 μm. C, Western blotting analyses showing the induction of cyclins in kidneys at days 3, 7 and 14 after UUO compared with sham control from CD-1 and C57BL/6 mice, respectively. D, Representative micrographs of immune staining showing the p-4E-BP1 positive cell in kidney tissues from C57BL/6 mice (upper panel), representative micrographs of immune staining showing the co-localization of p-4E-BP1 and p-Histone H3 in kidney tissues from C57BL/6 mice (lower panel). Scale bar, 50 μm.

3.3. Tubular epithelial cells transfected with dominant negative 4E-BP1 mutant rescues AA induced G2/M arrest and pro-fibrotic cytokine production

To access the importance of 4E-BP1 on TIF, pro-fibrotic cytokines and extracellular matrix were examined. NRK-52E cells were transfected with 4E-BP1A4 for 24 h. The mRNA level of TGF-β and CTGF were decreased after 4E-BP1A4 overexpression (Fig. 3D), so do the protein level of CTGF (Fig. 3E). And the expression of extracellular matrix FN was also suppressed (Fig. 3F).

Aristolochic acid nephropathy (AAN) is characterized by acute tubular necrosis, tubular atrophy, lymphocytic infiltrates and renal fibrosis [1], correlated with the arrest of proximal tubular epithelial cells in G2/M and the production of pro-fibrotic cytokines. To explore whether down-regulated p-4E-BP1 could decrease the production of pro-fibrotic cytokines and protect AKI, we performed AA to induce NRK-52E cells arrest in G2/M in vitro. NRK-52E cells were treated with 2 μM AA for 48 h, the expression of TGF-β, CTGF and FN were increased (Fig. 4A). AA significantly upregulated the protein level of Cyclin B1 and p-Histone H3 (Fig. 4B) and caused approximately 20.87% cells arrested in G2/M phase (Fig. 4C and D). Furthermore, the level of p-4E-BP1 was also increased (Fig. 4B), indicating that the phenomena induced by AA were associated with p-4E-BP1. And transfecting with 4E-BP1A4 for another 24 h, significantly reduced the pro-fibrotic cytokines production (Fig. 4A), Cyclin B1 and p-Histone H3 abundance (Fig. 4B) and decreased the G2/M arrested cell number (Fig. 4C–D). Together, these data indicate that decreasing the phosphorylation level of 4E-BP1 could protect kidney fibrosis.

3.4. Increased p-4E-BP1 is observed in the mitotic tubular epithelial cells in UUO kidneys

To investigate the role of 4E-BP1 in vivo, the level of p-4E-BP1 was examined in mice with UUO nephropathy (Fig. 5A and B). In order to exclude the influence of mouse breeds difference on mTOR signal, we generated UUO model in CD1 and C57BL/6 mice, respectively. Western blot showed that the UUO kidneys developed fibrosis at 14 days after operation in both two mice breeds (Fig. 5A), and PAS staining showed that there was no significant difference in the degree of tubular injury and histological change (Fig. 5B) between these two breeds at 14 days after UUO operation. While the mTORC2 pathway showed similar expression pattern between these two mice breeds, the level of p-S6 in CD1 mice reached the peak at day 3 after operation, and the abundance of p-S6 in C57BL/6 mice was continuously increased within day 14 after UUO operation. These results suggest that the signal variation are not uniform in different mice breeds.

p-4E-BP1 level was significantly increased within day 14, in either the CD-1 mice UUO kidneys or the C57BL/6 mice UUO kidneys (Fig. 5A and C). Similarly, in C57BL/6 mice, the level of Cyclin B1 and p-Histone H3 did not increased significantly until day 14. However, the levels of Cyclin B1 and p-Histone H3 were significantly increased from day 7 to day 14 in CD-1 mice (Fig. 5C). So the UUO kidneys from C57BL/6 mice were choose for further study. Immunostaining showed that increased p-4E-BP1 was located in tubular cells (Fig. 5D, upper panel), and it was co-localized with increased p-Histone H3 (Fig. 5D, lower panel). Therefore, it is concluded that the phosphorylation of 4E-BP1 regulates the cell cycle in tubular epithelia cells.

4. Discussion

We report here that in UUO model, p-4E-BP1 is accumulated in proximal tubular cells and arrested at G2/M. The expressions of Cyclin B1 and p-Histone H3 are downregulated in NRK-52E cells transfected with 4E-BP1 phosphorylation site mutation 4E-BP1A4, resulting in decreased G2/M phase cell number and pro-fibrosis factor production and rescuing the G2/M arrest induced by AA. Thus, this study indicates that downregulating p-4E-BP1 level in proximal tubular cells may protect kidney against AKI.

mTORC1 controls cell growth and proliferation by 4E-BPs and S6K [20]. It is generally accepted that S6K controls the cell growth, and 4E-BP1 regulates the cell proliferation, while ablation of S6 in mouse hepatocytes inhibits cell proliferation after partial hepatectomy [21,22], demonstrating that the functions of S6 are distinct in different cell types, so it is quite necessary to explore the function of S6 and 4E-BP1 in epithelial cells. In renal carcinoma cells, mTORC1 inhibited by rapamycin leads to G0/G1 arrest; however, rapamycin only partially inhibit the phosphorylation of 4E-BP1, but completely suppress the phosphorylation of S6 in a short time [14]. In this study, using 4E-BP1A4 to specifically down-regulate p-4E-BP1 causes a reduction in cell proliferation and decline in G2/M phase cell number, which does not affect the phosphorylation of S6. Hence, we report that, rather than S6K, 4E-BP1 controls the cell proliferation and cell cycle in tubular epithelial cells.

Additionally, in oocytes, p-4E-BP1 (Thr37/46, Ser65 and Thr70) shows no signal in the GV stage (germinal vesicle-nucleus in the oocyte) and is significantly enhanced from NEBD stage (nuclear envelope breakdown) to the metaphase of first or second meiotic maturation [23]. While, in this study, the immunohistochemistry image shows that the enhanced signal of p-4E-BP1 is located in the divided proximal tubular cells, which indicates that increased p-4E-BP1 could be countable for the increased epithelial proliferation in kidney injury; however, the causal relationship between the increase in p-4E-BP1 level and the increased cell proliferation is still unclear.

It is shown that Cyclin B is synthesized in late G2 and degraded during late M phase before the cells exit mitosis. Cells can escape from mitotic arrest, even in the presence of an unsatisfied spindle assembly check-point [24,25], through APC/C-dependent ubiquitination and proteolysis of cyclin B during mitotic slippage [26]. In this study, the abundance of Cyclin B1 is decreased after the dominant negative 4E-BP1 mutant is expressed, and the G2/M cells number is reduced. Hence, it is concluded that down-regulating the phosphorylation of 4E-BP1 contributes to cells escaping from mitosis, but not the transition of G2 to M phase. 4E-BP1 is a key component in cap-dependent translation which predominantly utilizes mRNA with TOP motif [27], and reduced phosphorylation of 4E-BP1 adversely affects translation [23]. However, it is still unclear whether the decreased Cyclin B1 expression is due to the decreased translation by p-4E-BP1 suppression or the increased APC/C-dependent proteolysis, and further investigations are required to confirm this.

5. Conclusion

In summary, this study demonstrates a new mechanism that p-4E-BP1 modulates the progression of TIF, via regulating the epithelial cell cycle.

Statement of author contributions

Xiaoli Sun performed the experiments and wrote the manuscript. Wei Wei, Jiafa Ren performed experiment and analyzed the data. Yan Liang, Mingjie Wang, Yuan Gui and Xian Xue revised the manuscript. Chunsun Dai and Jianzhong Li designed, supervised and revised the manuscript.

Acknowledgements

This work was supported by National Science Foundation of China grants (81700589) and Natural Science Foundation of Jiangsu Province (Grants NO BK 20170359).

References

[1] F.D. Debelle, J.L.L. Nortier, E.G. Prez De, C.H. Garbar, A.R. Vienne, I.J. Salmon, M.M. Deschodt-Lanckman, V. Jean-Louis, Aristolochic acids induce chronic renal failure with interstitial fibrosis in salt-depleted rats, J. Am. Soc. Nephrol. 13 (2002) 431–436 https://jasn.asnjournals.org/content/13/2/431.

[2] W.C. Burns, P. Kantharidis, M.C. Thomas, The role of tubular epithelial-mesenchymal transition in progressive kidney disease, Cells Tissues Organs 185 (2007) 222–231, https://doi.org/10.1159/000101323.

[3] F.T. Borges, S.A. Melo, Ö. BC, N. Kato, I. Revuelta, C.A. Miller, V.S. Lebleu, R. Kalluri, TGF-β1-containing exosomes from injured epithelial cells activate fibroblasts to initiate tissue regenerative responses and fibrosis, J. Am. Soc. Nephrol. 24 (2013) 385–392, https://doi.org/10.1681/ASN.2012101031.

[4] Y. Feng, J. Ren, Y. Gui, W. Wei, B. Shu, Q. Lu, X. Xue, X. Sun, W. He, J. Yang, C. Dai, Wnt/beta-catenin-promoted macrophage alternative activation contributes to kidney fibrosis, J. Am. Soc. Nephrol. 29 (2018) 182–193, https://doi.org/10.1681/ASN.2017040391.

[5] D.P. Basile, The endothelial cell in ischemic acute kidney injury: implications for acute and chronic function, Kidney Int. 72 (2007) 151–156, https://doi.org/10.1038/sj.ki.5002312.

[6] K. Raghu, N. Eric, Epithelial-mesenchymal transition and its implications for fibrosis, J. Clin. Invest. 112 (2003) 1776, https://doi.org/10.1172/JCI20530.

[7] S. Lovisa, V.S. Lebleu, B. Tampe, H. Sugimoto, K. Vadnagara, J.L. Carstens, C.C. Wu, Y. Hagos, B.C. Burckhardt, T. Pentchevahoang, Epithelial-to-mesenchymal transition induces cell cycle arrest and parenchymal damage in renal fibrosis, Nat. Med. 21 (2015) 998–1009, https://doi.org/10.1038/nm.3902.

[8] L. Yang, T.Y. Besschetnova, C.R. Brooks, J.V. Shah, J.V. Bonventre, Epithelial cell cycle arrest in G2/M mediates kidney fibrosis after injury, Nat. Med. 16 (2010) 535–543 531p following 143 https://doi.org/10.1038/nm.2144.

[9] M. Jiang, Z. Dong, Regulation and pathological role of p53 in cisplatin nephrotoxicity, J. Pharmacol. Exp. Ther. 327 (2008) 300–307, https://doi.org/10.1124/jpet.108.139162.

[10] P.M. Price, R.L. Safirstein, J. Megyesi, The cell cycle and acute kidney injury, Kidney Int. 76 (2009) 604–613, https://doi.org/10.1038/ki.2009.224.

[11] B. Magnuson, B. Ekim, D.C. Fingar, Regulation and function of ribosomal protein S6 kinase (S6K) within mTOR signalling networks, Biochem. J. 441 (2012) 1–21, https://doi.org/10.1042/BJ20110892.

[12] C. Porta, R.A. Figlin, Phosphatidylinositol-3-kinase/Akt signaling pathway and kidney cancer, and the therapeutic potential of Phosphatidylinositol-3-kinase/Akt inhibitors, J. Urol. 182 (2009) 2569–2577, https://doi.org/10.1016/j.juro.2009.08.085.

[13] R.J. Dowling, I. Topisirovic, T. Alain, M. Bidinosti, B.D. Fonseca, E. Petroulakis, X. Wang, O. Larsson, A. Selvaraj, Y. Liu, S.C. Kozma, G. Thomas, N. Sonenberg, mTORC1-mediated cell proliferation, but not cell growth, controlled by the 4E-BPs, Science 328 (2010) 1172–1176, https://doi.org/10.1126/science.1187532.

[14] H. Ito, O. Ichiyanagi, S. Naito, V.N. Bilim, Y. Tomita, T. Kato, A. Nagaoka, N. Tsuchiya, GSK-3 directly regulates phospho-4EBP1 in renal cell carcinoma cell-line: an intrinsic subcellular mechanism for resistance to mTORC1 inhibition, BMC Cancer 16 (2016), https://doi.org/10.1186/s12885-016-2418-7.

[15] L. Jiang, L. Xu, J. Mao, J. Li, L. Fang, Y. Zhou, W. Liu, W. He, A.Z. Zhao, J. Yang, C. Dai, Rheb/mTORC1 signaling promotes kidney fibroblast activation and fibrosis, J. Am. Soc. Nephrol. 24 (2013) 1114–1126, https://doi.org/10.1681/ASN.2012050476.

[16] F. Grahammer, S.K. Ramakrishnan, M.M. Rinschen, A.A. Larionov, M. Syed, H. Khatib, M. Roerden, J.O. Sass, M. Helmstaedter, D. Osenberg, L. Kühne, O. Kretz, N. Wanner, F. Jouret, T. Benzing, F. Artunc, T.B. Huber, F. Theilig, mTOR regulates endocytosis and nutrient transport in proximal tubular cells, J. Am. Soc. Nephrol. 28 (2017) 230–241.

[17] X.L. Sun, J.F. Yuan, T. Jin, X.Q. Cheng, Q. Wang, J. Guo, W. Zhang, Y. Zhang, L. Lu,

Z. Zhang, Physical and functional interaction of Snapin with Cav1.3 calcium channel impacts channel protein trafficking in atrial myocytes, Cell. Signal. 30 (2017) 118–129 http://www.ncbi.nlm.nih.gov/pubmed/27915047.
[18] J. Li, J. Ren, X. Liu, L. Jiang, W. He, W. Yuan, J. Yang, C. Dai, Rictor/mTORC2 signaling mediates TGFβ1-induced fibroblast activation and kidney fibrosis, Kidney Int. 88 (2015) 515–527, https://doi.org/10.1038/ki.2015.119.
[19] Y. Gui, J. Li, Q. Lu, Y. Feng, M. Wang, W. He, J. Yang, C. Dai, Yap/Taz mediates mTORC2-stimulated fibroblast activation and kidney fibrosis, J. Biol. Chem. 293 (2018) 16364–16375 https://www.ncbi.nlm.nih.gov/pubmed/30154246.
[20] D.A. Guertin, D.M. Sabatini, Defining the role of mTOR in cancer, Cancer Cell 12 (2007) 9–22, https://doi.org/10.1016/j.ccr.2007.05.008.
[21] S. Fumagalli, C.A. Di, A. Neb-Gulati, F. Natt, S. Schwemberger, J. Hall, G.F. Babcock, R. Bernardi, P.P. Pandolfi, G. Thomas, Absence of nucleolar disruption after impairment of 40S ribosome biogenesis reveals an rpL11-translation-dependent mechanism of p53 induction, Nat. Cell Biol. 11 (2009) 501–508, https://doi.org/10.1038/ncb1858.
[22] S. Volarevic, M.J. Stewart, B. Ledermann, F. Zilberman, L. Terracciano, E. Montini, M. Grompe, S.C. Kozma, G. Thomas, Proliferation, but not growth, blocked by conditional deletion of 40S ribosomal protein S6, Science 288 (2000) 2045–2047, https://doi.org/10.1126/science.288.5473.2045.
[23] D. Jansova, M. Koncicka, A. Tetkova, R. Cerna, R. Malik, L.E. Del, M. Kubelka, A. Susor, Regulation of 4E-BP1 activity in the mammalian oocyte, Cell Cycle 16 (2017) 927–939, https://doi.org/10.1080/15384101.2017.1295178.
[24] D.A. Brito, C.L. Rieder, Mitotic checkpoint slippage in humans occurs via cyclin B destruction in the presence of an active checkpoint, Curr. Biol. 16 (2006) 1194–1200, https://doi.org/10.1016/j.cub.2006.04.043.
[25] P.R. Andreassen, S.N. Martineau, R.L. Margolis, Chemical induction of mitotic checkpoint override in mammalian cells results in aneuploidy following a transient tetraploid state, Mutat. Res. 372 (1996) 181, https://doi.org/10.1089/089277902753483745.
[26] Y.Y. Park, J.-H. Ahn, M.-G. Cho, J.-H. Lee, ATP depletion during mitotic arrest induces mitotic slippage and APC/CCdh1-dependent cyclin B1 degradation, Exp. Mol. Med. 50 (2018), https://doi.org/10.1038/s12276-018-0069-2.
[27] K.C. Hopkins, M.A. Tartell, C. Herrmann, B.A. Hackett, F. Taschuk, D. Panda, S.V. Menghani, L.R. Sabin, S. Cherry, Virus-induced translational arrest through 4EBP1/2-dependent decay of 5'-TOP mRNAs restricts viral infection, Proc. Natl. Acad. Sci. U. S. A. 112 (2015) E2920, https://doi.org/10.1073/pnas.1418805112.